International Journal of Power Electronics and Drive System (IJPEDS)
Vol. 17, No. 2, June 2026, pp. 1440~1450
ISSN: 2088-8694, DOI: 10.11591/ijpeds.v17.i2.pp1440-1450

Adaptive control of the virtual synchronous generator by deep neural networks for a wind high power conversion chain

Wijdane El Maataoui, Abdelouahed Abounada
Team of Automatic and Energy Conversion, Faculty of Sciences and Technology, Sultan Moulay Slimane University, Beni Mellal, Morocco

Article Info

Article history:

Received Oct 1, 2025
Revised Apr 2, 2026
Accepted Apr 23, 2026

Keywords:

Adaptive control
Artificial neural network
End-to-end control
Inverter control
Supervised learning
Virtual synchronous generator
Wind turbine conversion system

ABSTRACT

The virtual synchronous generator (VSG) is commonly used to reproduce the inertial response of conventional synchronous machines. However, the VSG control architecture relies on controller chains, benchmark transformations, and parameter settings, including virtual inertia and damping, which limit its flexibility in highly dynamic environments. This paper proposes an innovative end-to-end control approach based on a neural network to fully replace the classical VSG control structure. The neural network developed is trained to directly generate inverter control signals from real-time electrical measurements, including voltages and currents, as well as active and reactive power. A dataset is generated from a detailed VSG model under different operating conditions, and then a multilayer neural network is trained using supervised learning with MATLAB. The resulting model is then integrated into a complete wind energy conversion chain simulated in Simulink. The simulation results demonstrate that control based on artificial neural networks ensures better frequency and voltage stability, more accurate tracking of the active power injected, and a significant improvement in power quality, with total harmonic distortion (THD) reduced to 0.04%, compared to 0.51% for conventional VSG control. These results confirm the potential of artificial intelligence-based approaches for the intelligent control of renewable energy systems.

Corresponding Author:

Wijdane El Maataoui
Team of Automatic and Energy Conversion, Faculty of Sciences and Technology
Sultan Moulay Slimane University
Beni Mellal, Morocco
Email: wijdane.elmaataoui@usms.ma

1. INTRODUCTION

The extensive integration of renewable energy sources, particularly wind power, has transformed modern power grids, with global cumulative wind power capacity reaching around 1 136 GW by the end of 2024 [1]. These generation sources are often connected to the grid via permanent magnet synchronous generators (PMSGs) and power converters to ensure an injection that meets the requirements of the power grid [2], [3]. In this context, the concept of the virtual synchronous generator (VSG) has emerged as an effective solution for artificially reproducing the inertia of synchronous machines by injecting a calculated inertial response [4]-[6].

The classic VSG structure is based on the swing equation, combined with voltage and reactive power regulation by Q-V or frequency and active power regulation P-f loops, followed by sinusoidal pulse width modulation (SPWM) [7]. Although this architecture is robust and based on established physical models, it has several limitations, including the need for accurate grid and machine modeling, which is

challenging in unstable or changing environments [8]. In addition, this approach is sensitive to proportional-integral (PI) controller tuning errors, the alignment of abc/dq Park transforms, and the quality of frequency filtering [9]. Parameters such as virtual inertia J or damping factor Dp are generally fixed, which reduces the system's adaptability [10].

Recently, artificial neural networks (ANNs) have demonstrated their effectiveness in modeling nonlinear systems, dynamic prediction, and command generation in complex contexts [11], [12]. In particular, several works have proposed neural models to dynamically adjust VSG parameters [13] or to replace certain control blocks with learned submodels [14]. However, few works go so far as to replace the entire VSG architecture with a single neural model, capable of directly generating inverter control pulses from local electrical measurements.

In this study, we propose direct end-to-end control using a supervised neural network. By generating a dataset via simulation in Simulink, we train a neural model in MATLAB. This model learns to associate the electrical states of the system with the control pulses required for direct current (DC)/alternating current (AC) conversion. This model is then integrated into a complete wind turbine conversion chain and compared with a conventional VSG control system in terms of stability, frequency response, and harmonic distortion criteria. Unlike previous hybrid ANN-VSG approaches that only replace or tune specific control loops, the proposed method performs a complete neural substitution of the VSG structure, enabling a simplified and adaptive controller suitable for real-time and embedded implementation.

2. WIND ENERGY CONVERSION CHAIN

Figure 1 illustrates the wind energy conversion chain, which includes the wind turbine, the PMSG, and the three-phase rectifier. It also consists of a chopper equipped with maximum power point tracking (MPPT), optimal torque algorithm control, and a DC bus. Additionally, the system incorporates a two-level three-phase inverter with VSG control, an LCL filter, and the three-phase grid [15].

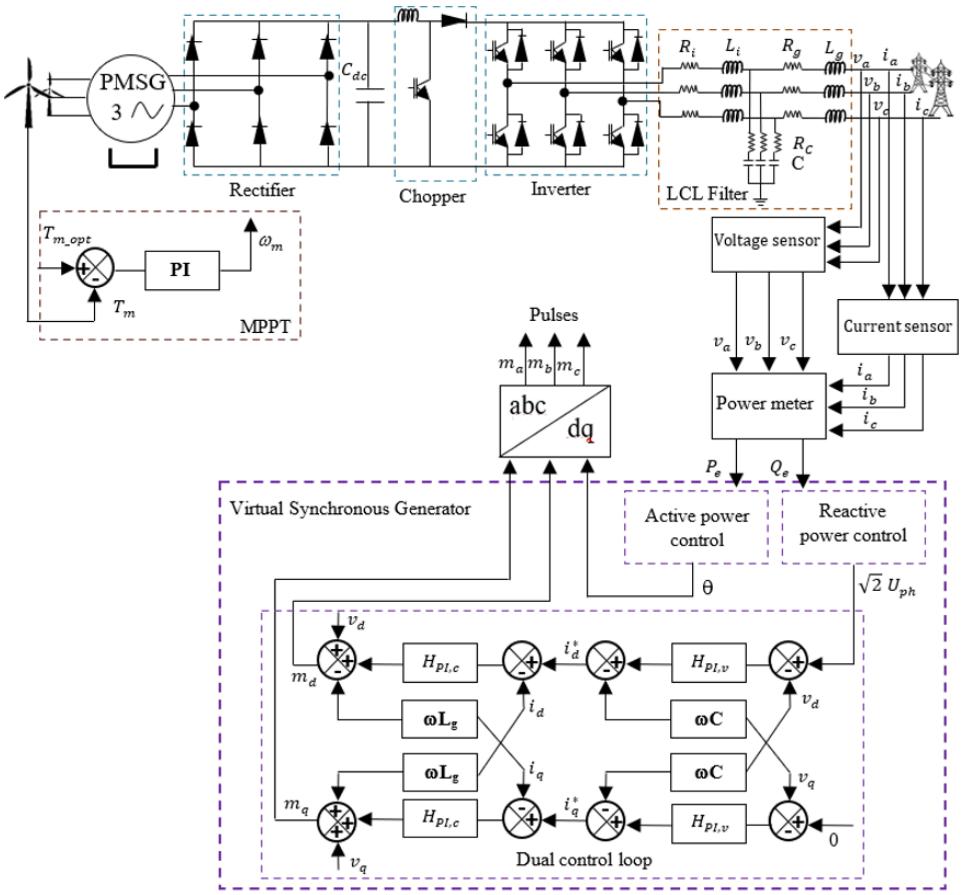

Figure 1. Diagram of the VSG control system integrated into the wind turbine conversion chain

3. CLASSICAL VSG

VSG control aims to reproduce the dynamic equations of a rotating synchronous machine.

3.1. Virtual inertia equation

Swing's equation, after applying the fundamental principle of dynamics to a rotating mass, is as (1).

$$J\alpha_m = \sum C_i = C_m - C_e \quad (1)$$

Where J is the total moment of inertia, α_m is the angular acceleration of the rotor, C_e is the electrical torque, and C_m is the mechanical torque. Depending on the power and damping terms of the synchronous machine, the swing becomes as (2) [15].

$$J\omega_m \frac{\mathrm{d}\omega_m}{dt} = P_m - P_e - D_p(\omega_m - \omega_{\mathrm{ref}}) \quad (2)$$

Where ω_m is the rotational speed, P_m is the active mechanical power, P_e is the electrical power, D_p is the damping factor, and ω_{ref} is the reference angular velocity.

3.2. Voltage and reactive power control

Voltage control improves stability and prevents current spikes. At the neutral point of the inverter, the voltage is given by (13) [16].

$$\sqrt{2}U_{ph} = G(s)\left(\sqrt{2}U_{ref} - \sqrt{2}U_n\right) \quad (3)$$

Where U_{ref} is the inverter reference voltage, and U_{ph} is the inverter phase voltage. The relationship between reactive power and voltage is given (4).

$$D_q\sqrt{2}\left(U_n - U_{ref}\right) = Q_e - Q_{ref} \quad (4)$$

Where D_q is the droop coefficient of reactive power and voltage, Un is the output voltage, Q_e is the reactive power, and Q_{ref} is the reference reactive power. By integrating $F(s) = D_q/sk_i$, the (4) becomes (5) [15].

$$\sqrt{2}E_{ph} = \frac{1}{k_i s}\left(Q_e - Q_{ref} + D_q\left(\sqrt{2}U_n - \sqrt{2}U_{ref}\right)\right) \quad (5)$$

3.3. Voltage and current loops

To further improve voltage and current outputs, two loops have been added: an internal current loop and an external voltage loop.

3.3.1. Voltage control

The DC circuit of the inverter is represented by (6) [17], [18].

$$C_{DC}\frac{dv}{dt} = i - i_{inv} \quad (6)$$

v_q^* is equal to zero, assuming that the 'd' axis is parallel to the AC mains voltage.

$$\begin{bmatrix} i_d^* \\ i_q^* \end{bmatrix} + C\omega \begin{bmatrix} v_d \\ v_q \end{bmatrix} = \left(\frac{1}{R_C} + \frac{C_{DC}}{s}\right)\begin{bmatrix} v_d^* - v_d \\ v_q^* - v_q \end{bmatrix} \quad (7)$$

With i_d^* and i_q^* corresponding respectively to the components of the output current along the d and q axes. (C) The capacitance of the filter capacitor. v_d and v_q are the components of the output voltage along the d and q axes, respectively. v_d^* and v_q^* correspond respectively to the components of the DC bus reference voltage along the d and q axes.

3.3.2. Current control

The voltages on the grid side of the power conversion chain are expressed in terms of the parameters of the LCL filter and the common coupling point representing the three-phase inverter as (8) [17], [18].

$$\begin{cases} m_d - v_d + \omega L_g i_q = \left(R_g + \frac{L_g}{s}\right)(i_d^* - i_d) \\ m_q - v_d - \omega L_g i_d = \left(R_g + \frac{L_g}{s}\right)(i_d^* - i_d) \end{cases} \quad (8)$$

Where m_d and m_q are the output reference values of the d and q axes of the current loop. v_d and v_q are the d- and q-axis voltage components of the common coupling point, respectively. L_g and R_g are the inductor and resistor of the mains-side filter, and ω is the angular frequency of the mains voltage. And i_d, i_q, i_d^*, and i_q^* indicate the d- and q-axis components of the mains-side currents and the reference output currents of the voltage loop, respectively.

3.4. Limits of classical control

Conventional VSG control, while emulating the behavior of a synchronous machine, suffers from several major limitations, making it ineffective in dynamic environments, such as microgrids with high penetration of renewable energies. Its fundamental parameters (virtual inertia J and damping coefficient D_p) are generally fixed, preventing it from adapting to rapid variations in the grid (load changes, voltage/frequency fluctuations), which can lead to inadequate or unstable response [19].

The sensitivity of its PI controllers requires fine-tuning, often heuristically, otherwise overshoot, oscillation, or slow response may occur, particularly during network disturbances [20]. Its computational complexity, due to multiple coordinate transformations and nested control loops, can add to the real-time load on embedded platforms. In addition, it lacks mechanisms for dynamic adaptation to sudden changes in the environment, such as grid voltage variations or load disconnection. Dependence on accurate system modeling also compromises performance in the presence of uncertainties or non-linearities that are not taken into account [21]. Finally, conventional VSG control takes no advantage of historical data or past system behavior, acting without predictive capability or adaptive learning, unlike more recent approaches based on artificial intelligence or adaptive control [22].

4. SUPERVISED NEURAL NETWORK

The proposed approach aims to replace conventional VSG control with a supervised neural network capable of directly generating inverter control signals from measured electrical quantities. This methodology relies on supervised learning techniques. It is structured into three main stages: data generation, model training, and integration into the converter chain [23].

4.1. Dataset generation

A crucial step in training a high-performance neural network is the creation of a high-quality training dataset. In our case, this training data is generated from a VSG model simulated in MATLAB/Simulink [24], [25]. At each point in the simulation, the input variables of the future neural network are measured. These are the system's key electrical quantities: voltages in the d_q frame (v_d, v_q), stator currents in the d_q frame (i_d, i_q), injected active power (P_e), and injected reactive power (Q_e). At the same time, the corresponding output signals, which serve as 'ground truth', are collected. These signals are the PWM pulses generated by the SPWM modulator of the classic VSG.

4.2. Neural network training

Training the artificial neural network involves using the data collected by a supervised learning model. It aims to form a direct non-linear mapping between inputs and outputs, in this case, the six measured electrical quantities and the PWM pulse signals. The neural network used in this study is the multi-layer perceptron (MLP), which is represented by a feedforward architecture widely used for regression and classification tasks [26], [27]. The architecture of the MLP is shown in Figure 2.

Non-linearity is introduced by applying an activation function [28] to the weighted sums of the inputs of each neuron in the hidden layers and the output layer. The network is trained using the 'fitnet' function in MATLAB. This function is used to configure and train a feedforward neural network for regression tasks. The Levenberg-Marquardt algorithm [29] is generally used for this function. It combines the fast convergence near the minimum of the Gauss-Newton method and the robustness far from the minimum of gradient descent, for improved nonlinear optimization.

The training steps are shown in Figure 3, with the initialization of the connection coefficients between neurons (weights) and the values added to the weighted sum of inputs (bias) [30]. This is a crucial step in enabling the network to learn different features. Next, forward propagation is used to transmit the input data through the network layers. Application of an activation function to the weighted sum of inputs produces the neural outputs [31]. The error calculation is a comparison between the output generated by the neural network and the output of the 'ground-truth' VSG model [32].

In this case, to quantify the difference between predicted and actual output, a cost function such as the mean squared error (MSE) is calculated. The calculated error is propagated from the output layer to the input layer through the neural network. The backpropagation algorithm minimizes the cost function by calculating the gradients of this function to each weight and bias of the network, indicating the necessary adjustments. This algorithm is called backpropagation [33], and it calculates the gradients of the cost function concerning each weight and bias in the network, indicating the necessary adjustments. Afterwards, an update is applied to find the weights and biases that enable more accurate prediction of PWM pulses [34].

Once the error reaches a 10^{-6} threshold, or performance no longer improves on a separate validation set, the repetition process on the 'epoch' training data set is stopped. To prevent overfitting, it is necessary to use a validation set. This occurs when the model loses its ability to generalize to unseen data, even if it learns the training data too well.

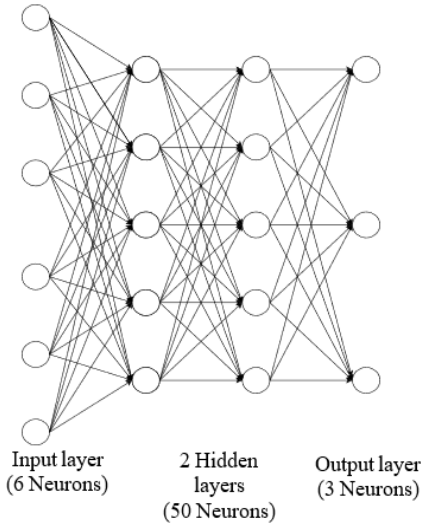

Figure 2. MLP architecture

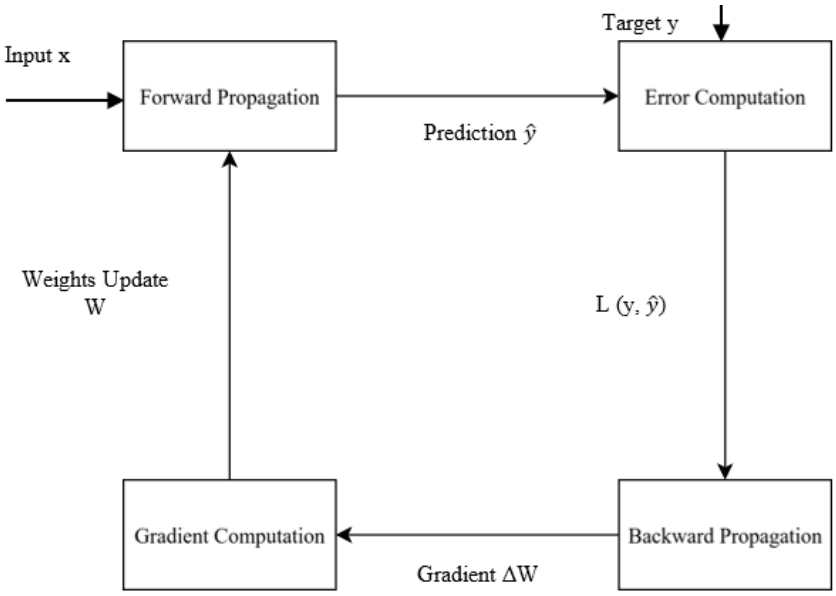

Figure 3. Supervised training process for a neural network, including forward propagation, error calculation, backpropagation, and weight updating

4.3. Neural model integration

Once trained and validated, the artificial neural network is integrated into the wind energy conversion chain to replace conventional VSG control, as shown in Figure 4. This 'end-to-end' approach consists of generating PWM pulses from electrical ratings measured in real time, using the network's learning capabilities [35]. This integration offers several significant advantages, such as simplification of the control structure, as the neural network replaces a complex set of controllers, transformations, and modulation modules, which can reduce the computational load and complexity of implementation on embedded platforms, once the model has been trained [22], [36]. Increased adaptability and robustness, having been trained on a variety of scenarios, the neural network can intrinsically adapt to network variations and disturbances, without requiring manual adjustments or explicit adaptation mechanisms for each parameter [37].

It can handle non-linearities and model uncertainties that conventional controllers struggle to address [38]. With improved dynamic responsiveness, the neural network's ability to process information in parallel and generate direct commands can potentially lead to faster response times and better transient system performance [39]. Integration of the neural model in Simulink enables rigorous validation of its performance in a complete system environment by directly comparing its behavior with that of conventional VSG control.

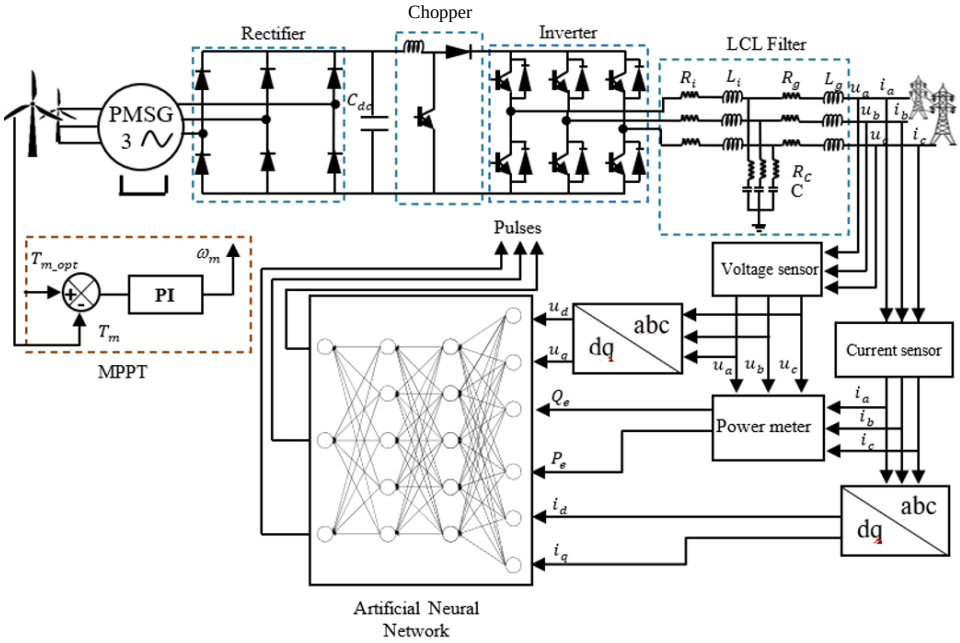

Figure 4. Integration of the trained neural network in the energy conversion chain, replacing the conventional VSG control

5. RESULTS AND DISCUSSION

The performance of the neural network control was evaluated and compared with that of the conventional VSG control through simulations in MATLAB/Simulink. Figure 5 shows the rapid and stable convergence of the neural network. After approximately 200 iterations, the MSE decreases significantly, demonstrating effective learning. The curves associated with the training, validation, and test sets remain parallel, indicating generalization without overfitting. The stability, robustness, and accuracy of the trained network demonstrate its relevance as an alternative to conventional VSG control.

Figure 6 shows a comparison between two control strategies: Figure 6(a) conventional VSG control and Figure 6(b) neural network-based control. In the case of conventional VSG control, relatively large oscillations around the nominal frequency of 50 Hz can be observed. This behavior is due to fixed-gain controllers, whose performance is sensitive to initial parameters and network conditions.

In contrast, there is a significant reduction in the amplitude of oscillations, as well as a shorter stabilization time for neural network-based control. This strategy makes it possible to generate more appropriate control pulses in real time, without explicit dependence on rigid system modeling. These results confirm the value of the proposed end-to-end approach to replace conventional controllers in VSGs, while improving system stability and response time.

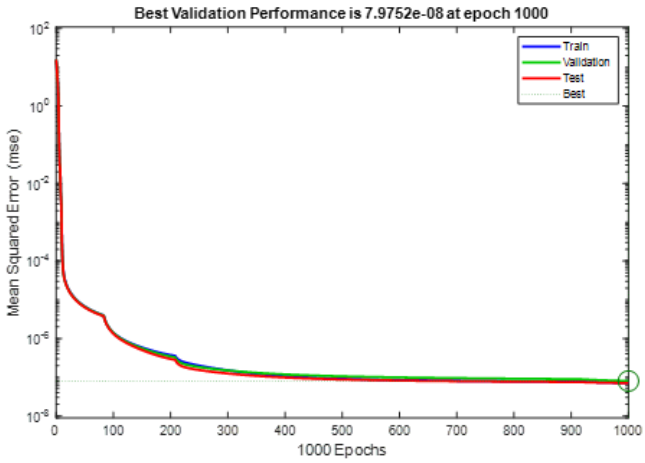

Figure 5. Neural network performance

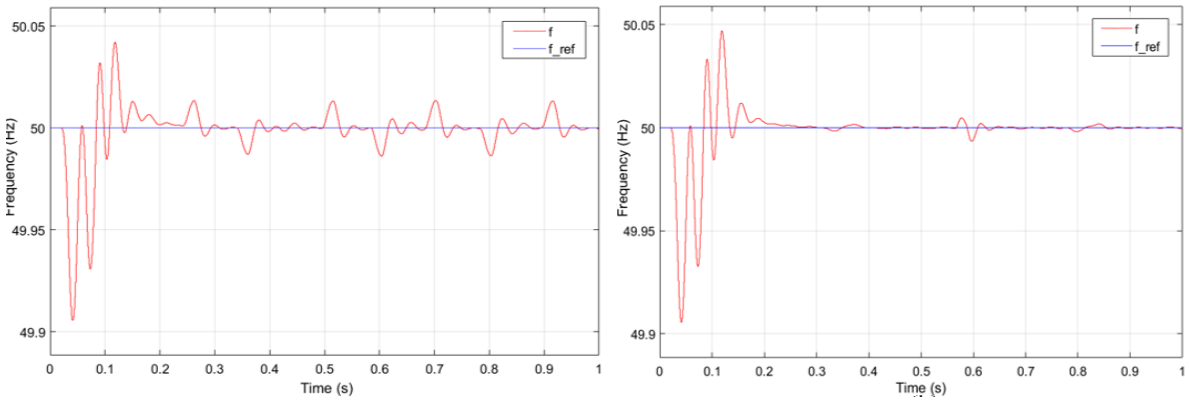

Figure 6. System frequency with (a) conventional VSG control and (b) neural network control

Figure 7 compares the active power injected by the system with Figure 7(a) conventional VSG control and Figure 7(b) neural network-based control. In both Figures, the power generally follows the 5 MW setpoint. For conventional VSG control, it can be seen that the active power injected shows more pronounced fluctuations around the setpoint due to the limitations of PI controllers. However, it can be seen that neural control provides better regulation. Oscillations around the setpoint are significantly reduced. This comparison shows that neural control is more stable and robust, which improves renewable energy production.

Figure 8 compares the output current quality for the two control strategies via a time and frequency analysis. Figure 8(a) conventional VSG control has a higher THD of 0.51%, with harmonic components visible in the Fourier spectrum. In contrast, Figure 8(b) the neural control has a sinusoidal output signal, with a very low THD of 0.04%. This performance indicates the remarkable ability of the neural network to generate appropriate control signals, minimizing distortion.

This comparison demonstrates the effectiveness of the neural network in improving output current quality and reducing harmonics while complying with grid connection conditions. Table 1 shows the general parameters of the system, including a nominal frequency of 50 Hz, which corresponds to the standard frequency of electrical networks. The active power injected is set at 5 MW, which represents a realistic scale for an industrial wind conversion application. The reactive power is zero, reflecting operation at a unity power factor. The high switching frequency of 10 kHz ensures fine modulation and good output signal quality.

Table 2 details the parameters of the output filter, which plays a key role in smoothing the signals output by the inverter and limiting the harmonics injected into the grid. The high values of the resistors and inductors on the inverter side reflect a pronounced filtering strategy to dampen high-frequency disturbances. On the grid side, the lower resistor and inductor values are intended to maintain the coupling dynamics with the fast grid. The filter's capacitance, combined with the damping resistor, ensures effective passive filtering and helps reduce harmonic distortion.

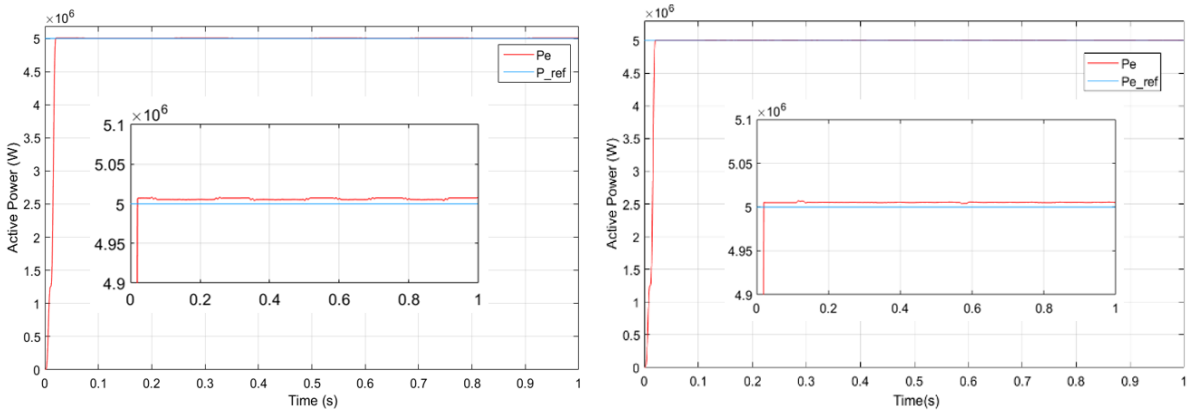

(a) (b)

Figure 7. Active power of the system with (a) conventional VSG control and (b) neural network control

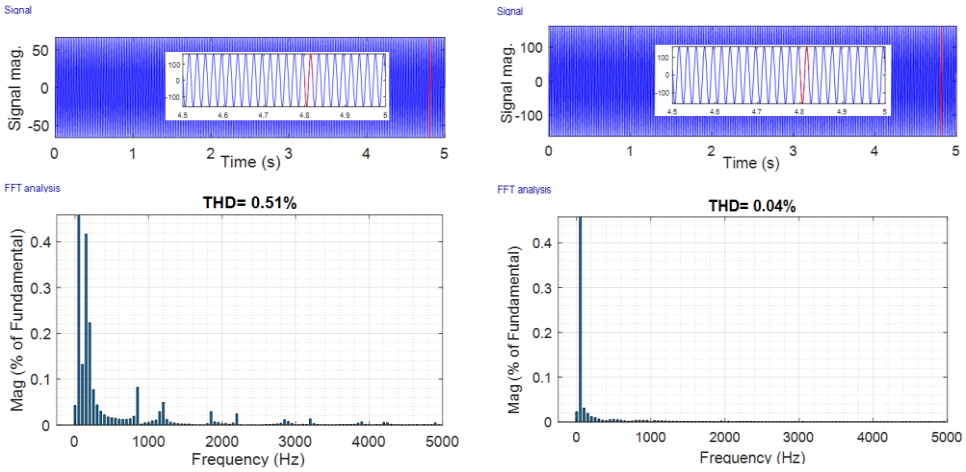

(a) (b)

Figure 8. Total harmonic distortion with (a) conventional VSG control and (b) neural network control

Table 1. System parameters

Parameters	Symbol	Value
Frequency	f	50 Hz
Active power	P	5 MW
Reactive power	Q	0 VA
Switching frequency	fsw	10 kHz

Table 2. Filter parameters

Parameters	Symbol	Value
Inverter side resistor	Ri	4373.03 Ω
Inverter side inductor	Li	0.033 H
Grid side resistor	Rg	174.93 Ω
Grid side inductor	Lg	5.676 µH
Damping resistor	RC	217.97 Ω
Capacity	C	8.544 mF

Table 3 summarizes the parameters of the PI controllers used in the various control loops, current voltage, and optimal torque. The kp and ki gains for voltage control are low, which is typical for systems with long time constants. The gains for current control are higher to enable a rapid response to load variations. The parameters for optimal torque control strike a good balance between responsiveness and stability in machine control, ensuring the efficient transfer of mechanical energy to electrical energy.

Table 3. Controllers' parameters

Parameters	Symbol	Value
Voltage control	kp	0.004587
	ki	0.0022
Current control	kp	1.7493
	ki	0.000005676
Optimal torque control	kp	0.00211
	ki	0.00448

6. CONCLUSION

This article proposes a new approach that involves replacing the conventional VSG control with an end-to-end neural network. This control is based on a supervised learning artificial neural network capable of generating the inverter control pulses, voltages, currents, and active and reactive power. The simulation results demonstrated the stability of frequency and active power, as well as a reduction in THD to 0.04% compared to 0.51% for conventional VSG control. In addition, the very low MSE showed a generalization of the neural network. These findings prove the robustness and flexibility of neural network-based control in the face of the limitations of conventional VSG control. This approach enables wind energy conversion systems to better meet grid connection requirements in terms of stability and power quality.

ACKNOWLEDGMENTS

The authors would like to thank the anonymous reviewers for their helpful and constructive comments that would greatly contribute to improving the final version of the paper. They would also like to thank the Editors for their generous comments and support.

FUNDING INFORMATION

The authors state no funding involved.

AUTHOR CONTRIBUTIONS STATEMENT

This journal uses the Contributor Roles Taxonomy (CRediT) to recognize individual author contributions, reduce authorship disputes, and facilitate collaboration.

Name of Author	C	M	So	Va	Fo	I	R	D	O	E	Vi	Su	P	Fu
Wijdane El Maataoui	✓	✓	✓	✓	✓	✓	✓	✓	✓	✓	✓		✓	✓
Abdelouahed Abounada		✓			✓					✓	✓	✓		

C : **C**onceptualization
M : **M**ethodology
So : **So**ftware
Va : **Va**lidation
Fo : **Fo**rmal analysis
I : **I**nvestigation
R : **R**esources
D : **D**ata Curation
O : Writing - **O**riginal Draft
E : Writing - Review & **E**diting
Vi : **Vi**sualization
Su : **Su**pervision
P : **P**roject administration
Fu : **Fu**nding acquisition

CONFLICT OF INTEREST STATEMENT

The authors state no conflict of interest.

DATA AVAILABILITY

The datasets generated during and/or analyzed during the current study are available from the corresponding author on reasonable request.

REFERENCES

[1] Global Wind Energy Council, "Wind industry installs record capacity in 2024 despite policy instability," GWEC, [Online]. Available: https://www.gwec.net/gwec-news/wind-industry-installs-record-capacity-in-2024-despite-policy-instability. [Accessed: Apr. 1, 2026].

[2] V. V. Yadav and S. Balasubramaniyan, "Synchronization stability and control strategies for PMSG-based wind energy systems under grid fault conditions," *Energy Reports*, vol. 13, pp. 6148–6160, Jun. 2025, doi: 10.1016/j.egyr.2025.05.052.

[3] Y. Zheng, Y. Xu, Y. Yang, L. Hua, and Y. Yang, "Application of adaptive virtual synchronous generator based on improved active power loop in photovoltaic storage systems," *Frontiers in Energy Research*, vol. 12, Jan. 2025, doi: 10.3389/fenrg.2024.1468629.
[4] C. Lu and X. Zhuan, "Adaptive control for virtual synchronous generator parameters based on soft actor critic," *Sensors*, vol. 24, no. 7, p. 2035, Mar. 2024, doi: 10.3390/s24072035.
[5] T. Shi, J. Sun, X. Han, and C. Tang, "Research on adaptive optimal control strategy of virtual synchronous generator inertia and damping parameters," *IET Power Electronics*, vol. 17, no. 1, pp. 121–133, Jan. 2024, doi: 10.1049/pel2.12620.
[6] L. Yang, X. Zhu, Y. Li, X. Chen, B. Huang, and Z. Xu, "Virtual synchronous control strategy and inertia analysis of large-scale energy storage," *Journal of Electric Power Science and Technology*, vol. 39, no. 2, pp. 190–197, 2024, doi: 10.19781/j.issn.1673-9140.2024.02.021.
[7] M. Yang, L. Zhang, X. Song, W. Kang, and Z. Kang, "A transient control strategy for grid-forming photovoltaic systems based on dynamic virtual impedance and RBF neural networks," *Electronics*, vol. 14, no. 4, p. 785, Feb. 2025, doi: 10.3390/electronics14040785.
[8] O. Babayomi, Y. Li, Z. Zhang, and K.-B. Park, "Advanced control of grid-connected microgrids: challenges, advances, and trends," *IEEE Transactions on Power Electronics*, vol. 40, no. 6, pp. 7681–7708, Jun. 2025, doi: 10.1109/TPEL.2025.3526246.
[9] J. Han, X. Feng, H. Zhao, P. Hu, and C. He, "Adaptive VSG control strategy considering energy storage SOC constraints," *Frontiers in Energy Research*, vol. 11, Sep. 2023, doi: 10.3389/fenrg.2023.1278648.
[10] F. Wang, L. Zhang, X. Feng, and H. Guo, "An adaptive control strategy for virtual synchronous generator," *IEEE Transactions on Industry Applications*, vol. 54, no. 5, pp. 5124–5133, Sep. 2018, doi: 10.1109/TIA.2018.2859384.
[11] Y. LeCun, Y. Bengio, and G. Hinton, "Deep learning," *Nature*, vol. 521, no. 7553, pp. 436–444, May 2015, doi: 10.1038/nature14539.
[12] I. S. Mohamed, S. Rovetta, T. D. Do, T. Dragicevic, and A. A. Z. Diab, "A neural-network-based model predictive control of three-phase inverter with an output LC Filter," *IEEE Access*, vol. 7, pp. 124737–124749, 2019, doi: 10.1109/ACCESS.2019.2938220.
[13] Q. Hu *et al.*, "Grid-forming inverter enabled virtual power plants with inertia support capability," *IEEE Transactions on Smart Grid*, vol. 13, no. 5, pp. 4134–4143, Sep. 2022, doi: 10.1109/TSG.2022.3141414.
[14] Y. Wang and R.-J. Wai, "Adaptive fuzzy-neural-network power decoupling strategy for virtual synchronous generator in micro-grid," *IEEE Transactions on Power Electronics*, vol. 37, no. 4, pp. 3878–3891, Apr. 2022, doi: 10.1109/TPEL.2021.3120519.
[15] W. El Maataoui, S. El Daoudi, A. Abounada, and M. Mabrouki, "A comparative study of virtual synchronous generator and sinusoidal pulse width modulation in a wind high power conversion chain," *Archives of Electrical Engineering*, vol. 73, no. 4, pp. 961–976, 2024, doi: 10.24425/aee.2024.152105.
[16] J. Liu, F. Rafi, J. Lu, and M. J. Hossain, "Neutral current compensation in a VSG-based three-phase four-wire microgrid system," in *2018 IEEE International Conference on Environment and Electrical Engineering and 2018 IEEE Industrial and Commercial Power Systems Europe (EEEIC / I&CPS Europe)*, Jun. 2018, pp. 1–6. doi: 10.1109/EEEIC.2018.8494488.
[17] W. El Maataoui, S. El Daoudi, L. Lazrak, and M. Mabrouki, "Improved performance of the grid side power conversion chain by adopting multilevel inverter topologies with an optimized LCL filter," in *Digital Technologies and Applications*, vol. 455, S. Motahhir and B. Bossoufi, Eds., in Lecture Notes in Networks and Systems, vol. 455., Cham: Springer International Publishing, 2022, pp. 507–515. doi: 10.1007/978-3-031-02447-4_52.
[18] W. El Maataoui, S. El Daoudi, L. Lazrak, and M. Mabrouki, "Minimized total harmonic distortion of a multi-level inverter of a wind power conversion chain synchronized to the grid-LCL filter optimization and third harmonic cancellation," ELECT, vol. 22, no. 1, pp. 27–40, Nov. 2021, doi: 10.5152/electrica.2021.21086.
[19] Z. Ling, Y. Liu, Z. Wang, and J. Yin, "Adaptive inertia and damping of grid-connected inverter with improved VSG control," *IET Power Electronics*, vol. 16, no. 16, pp. 2769–2781, Dec. 2023, doi: 10.1049/pel2.12600.
[20] M. A. Shobug, F. Yang, and J. Lu, "Stability improvement of microgrids under dynamic load conditions: A new adaptive virtual synchronous generator based virtual inertia control approach," *Results in Engineering*, vol. 25, p. 104556, Mar. 2025, doi: 10.1016/j.rineng.2025.104556.
[21] H. Grover, S. Sharma, A. Verma, M. J. Hossain, and I. Kamwa, "Adaptive parameter tuning strategy of VSG-based islanded microgrid under uncertainties," *Electric Power Systems Research*, vol. 235, p. 110854, Oct. 2024, doi: 10.1016/j.epsr.2024.110854.
[22] X. Ding and J. Cao, "Deep and reinforcement learning in virtual synchronous generator: a comprehensive review," *Energies*, vol. 17, no. 11, p. 2620, May 2024, doi: 10.3390/en17112620.
[23] Y. Li *et al.*, "Data-driven optimal control strategy for virtual synchronous generator via deep reinforcement learning approach," *Journal of Modern Power Systems and Clean Energy*, vol. 9, no. 4, pp. 919–929, 2021, doi: 10.35833/MPCE.2020.000267.
[24] Y. Lu *et al.*, "Machine learning for synthetic data generation: A review," *arXiv preprint* arXiv:2302.04062, Apr. 2025, doi: 10.48550/arXiv.2302.04062.
[25] C. R. Sticht and S. A. Bukowski, *Power system waveform datasets for machine learning*, Idaho National Laboratory, Idaho Falls, ID, USA, Rep. INL/RPT-23-76029-Rev000, 2024.
[26] J. Carmichael and Y. Liao, "Bayesian optimization of multi-layer perceptron models for power distribution system state estimation," *International Journal of Emerging Electric Power Systems*, vol. 25, no. 4, pp. 495–507, Aug. 2024, doi: 10.1515/ijeeps-2022-0328.
[27] M. Qiao, Y. Liang, A. Tavares, and X. Shi, "Multilayer perceptron network optimization for chaotic time series modeling," *Entropy*, vol. 25, no. 7, p. 973, Jun. 2023, doi: 10.3390/e25070973.
[28] I. Khalfaoui-Hassani and S. Kesselheim, "Polynomial, trigonometric, and tropical activations," *arXiv preprint* arXiv:2502.01247, Mar. 2026.
[29] J. J. Moré, "The Levenberg-Marquardt algorithm: Implementation and theory," 1978, pp. 105–116. doi: 10.1007/BFb0067700.
[30] M. V. Narkhede, P. P. Bartakke, and M. S. Sutaone, "A review on weight initialization strategies for neural networks," *Artificial Intelligence Review*, vol. 55, no. 1, pp. 291–322, Jan. 2022, doi: 10.1007/s10462-021-10033-z.
[31] S. R. Dubey, S. K. Singh, and B. B. Chaudhuri, "Activation functions in deep learning: A comprehensive survey and benchmark," *Neurocomputing*, vol. 503, pp. 92–108, Sep. 2022, doi: 10.1016/j.neucom.2022.06.111.

[32] J. Terven, D. M. Cordova-Esparza, J. A. Romero-González, A. Ramírez-Pedraza, and E. A. Chávez-Urbiola, "A comprehensive survey of loss functions and metrics in deep learning," *Artificial Intelligence Review*, vol. 58, no. 7, 2025, doi: 10.1007/s10462-025-11198-7.
[33] J. Li, J. Cheng, J. Shi, and F. Huang, "Brief introduction of back propagation (BP) neural network algorithm and its improvement," 2012, pp. 553–558. doi: 10.1007/978-3-642-30223-7_87.
[34] Z. Wu, M. Zhang, B. Fan, Y. Shi, and X. Guan, "Deep synchronization control of grid-forming converters: a reinforcement learning approach," *IEEE/CAA Journal of Automatica Sinica*, vol. 12, no. 1, pp. 273–275, Jan. 2025, doi: 10.1109/JAS.2024.124824.
[35] A. K. Thangapandi, A. Kumar, D. Karthigeyan, S. Ramasamy, V. Arumugam, and G. Gatto, "A novel artificial neural network based selection harmonic reduction technique for single source fed high gain switched capacitor coupled multilevel inverter for renewable energy applications," *Heliyon*, vol. 10, no. 19, 2024, doi: 10.1016/j.heliyon.2024.e38550.
[36] M. Chen *et al.*, "Power for AI and AI for power: The infinite entanglement between artificial intelligence and power electronics systems," *IEEE Power Electronics Magazine*, vol. 12, no. 1, pp. 37–43, Mar. 2025, doi: 10.1109/MPEL.2024.3524742.
[37] M. K. Rajak and R. Pudur, "Multiobjective adaptive predictive virtual synchronous generator control strategy for grid stability and renewable integration," *Scientific Reports*, vol. 15, no. 1, p. 9241, Mar. 2025, doi: 10.1038/s41598-025-93721-y.
[38] A. Mensah Akwasi, H. Chen, J. Liu, and O.-A. Duku, "Hybrid adaptive learning-based control for grid-forming inverters: real-time adaptive voltage regulation, multi-level disturbance rejection, and Lyapunov-based stability," *Energies*, vol. 18, no. 16, p. 4296, Aug. 2025, doi: 10.3390/en18164296.
[39] J. Zhou, S. Zhou, S. Chen, and Y. Sun, "Adaptive transient damping control strategy of VSG system based on dissipative hamiltonian neural network," *Electronics*, vol. 14, no. 11, p. 2207, May 2025, doi: 10.3390/electronics14112207.

BIOGRAPHIES OF AUTHORS

Wijdane El Maataoui is a researcher in the Team of Automatic and Energy Conversion, Faculty of Sciences and Technology, Sultan Moulay Slimane University, Beni Mellal, Morocco. She received her Electrical Engineering degree from Higher Normal School for Technical Education, Mohammedia, Morocco, in 2020. She has published in respected peer-reviewed journals and is involved in research on renewable energy conversion, control of power converters, and energy systems. She can be contacted at email: wijdane.elmaataoui@usms.ma.

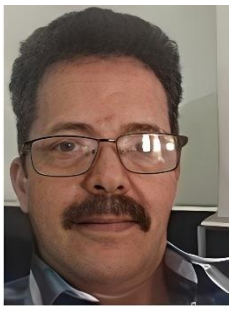

Abdelouahed Abounada received his B.Sc. degree from Cadi Ayyad University, Marrakech, Morocco, in 1989, and his Ph.D. degree in Automatic Control from the same university in 1992. He is currently a professor at Sultan Moulay Slimane University, Beni-Mellal, Morocco. His research interests include advanced methods for numerical automation, power electronics, and the integration of renewable energies into electrical systems. Abdelouahed is committed to advancing knowledge and technology in these fields to contribute to the development of sustainable energy solutions. He can be contacted at email: a.abounada@gmail.com.